

Attack of Substituted Alkynes on Olefin Palladium(0) Derivatives of Pyridylthioethers. The First Kinetic Study on the Mechanism of Formation of Palladacyclopentadiene Complexes

Luciano Canovese,^{*,†} Fabiano Visentin,[†] Gavino Chessa,[†] Paolo Uguagliati,[†] Carlo Levi,[†] and Alessandro Dolmella[§]

Dipartimento di Chimica, Università Ca' Foscari, Calle Larga S. Marta 2137, 30123 Venezia, Italy, and Dipartimento di Scienze Farmaceutiche, Università di Padova, Via F. Marzolo 5, 35131 Padova, Italy

Received June 21, 2005

The formation of metallacyclopentadienyl derivatives was studied under controlled conditions, and the kinetics and mechanism of reactions between pyridylthioether olefin Pd(0) substrates and substituted alkynes of the type $ZC\equiv CZ$ ($Z = COOMe, COOEt, COO^t\text{-Bu}$) leading to the corresponding palladacyclopentadienyl species were systematically investigated. In the case of less hindered ancillary ligands the attack of the alkyne forming a reactive monoalkyne intermediate was found to be the rate-determining step. In this respect the rates of reaction were discussed in terms of the substituent-induced basicity of sulfur and nitrogen of the ancillary ligands. The associative nature of the attack was unequivocally established, and the formation of a transition state bearing a monodentate ancillary ligand was proposed. In the case of more hindered ancillary ligands a partially stabilized monoalkyne intermediate is formed irrespective of the olefin in the starting complex, and this species strongly influences the reaction progress. Formation of hexamethylmellitate under mild conditions is also observed.

Introduction

Palladium-catalyzed reactions involving unsaturated molecules are well documented by the wealth of papers that have appeared in recent years. For instance, several annulation reactions¹ and the synthesis of conjugated dienes² represent two important and widely studied topics in which palladium substrates and alkynes react through the key intermediacy of metallacyclic complexes of palladium(II). The central role of these compounds is well recognized, and the chemistry of group 10 metallacycles was recently reviewed.³ However, despite their importance, no detailed mechanistic studies on the formation of these substrates are available in the literature since they were first synthesized by Maitlis in the 1970s by reacting Pd_2DBA_3 with dimethylacetylene dicarboxylate (DMA) in a variety of solvents to give the polymeric substrate $[Pd(CCOOMe)_4]_n$. The latter can be converted into several different derivatives including dienes, mellitates, and pallada-

cyclopentadienes by addition of the appropriate reactants.⁴ It was soon noticed that reactions of Pd_2DBA_3 with DMA carried out in the presence of an ancillary ligand (L) lead to the formation of palladacyclopentadiene complexes of the type $[PdL_2(CCOOMe)_4]$. However, the electronic features of ancillary ligands were important; thus, in the presence of phosphines or phosphites the derivatives containing π -coordinated DMA were separated, but only the phosphine substrate could add one further DMA molecule to give the palladacyclopentadiene species, the complex $[Pd(\eta^2\text{-DMA})L_2]$ (L = phosphites) being unreactive. The influence of the π -acidity of ancillary ligands was apparent, and cyclopalladate species only could be obtained when essentially dative ancillary ligands were employed.⁵

Ishii and co-workers also demonstrated that the complex $[Pd(\eta^2\text{-ma})(bipy)]$ (ma = maleic anhydride, bipy = 2,2'-bipyridyl) can easily add two DMA molecules, giving rise to the expected palladacyclopentadienyl species,⁵ but, to the best of our knowledge, no other Pd(0) substrates bearing different olefins or ancillary ligands were studied in order to assess whether the electronic and steric features of the chemical environment could influence the cyclometalation reaction path.

* To whom correspondence should be addressed. E-mail: cano@unive.it.

[†] Università Ca' Foscari.

[§] Università di Padova.

(1) (a) Schore, N. E. *Chem. Rev.* **1988**, 88, 1081. (b) Cacchi, S. *J. Organomet. Chem.* **1999**, 576, 42. (c) Rubin, M.; Sromek, A. W.; Gevorgyan V. *Synlett.* **2003**, 15, 2265.

(2) (a) van Belzen, R.; Hoffman, H.; Elsevier, C. J. *Angew. Chem., Int. Ed. Engl.* **1997**, 36, 1743. (b) van Belzen, R.; Klein, R. A.; Kooijman, H.; Veldman, N.; Spek, A. L.; Elsevier, C. J. *Organometallics* **1998**, 17, 1812. (c) van Belzen, R.; Elsevier, C. J.; Dedieu, A.; Veldman, N.; Spek, A. L. *Organometallics* **2003**, 22, 722.

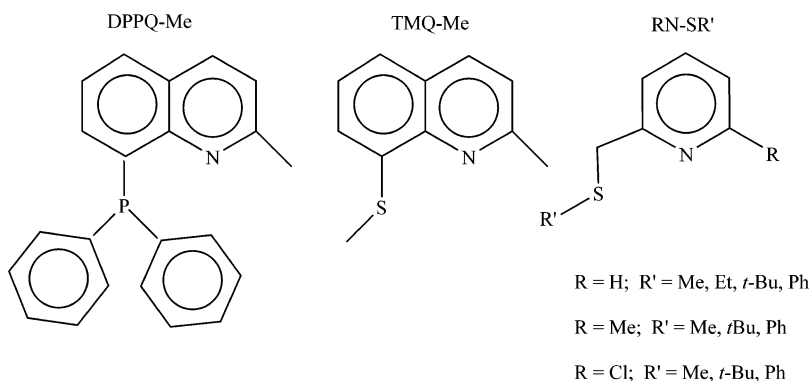
(3) Campora, J.; Palma, P.; Carmona, E. *Coord. Chem. Rev.* **1999**, 193–195, 207.

(4) (a) Moseley, K.; Maitlis, P. M. *Chem. Commun.* **1971**, 1604. (b) Roe, D. M.; Bailey, P. M.; Moseley, K.; Maitlis, P. M. *J. Chem. Soc., Chem. Commun.* **1972**, 1273. (c) Moseley, K.; Maitlis, P. M. *J. Chem. Soc. Dalton Trans.* **1974**, 169. (d) Roe, D. M.; Calvo, C.; Krishnamachari N.; Maitlis, P. M. *J. Chem. Soc., Dalton Trans.* **1975**, 125.

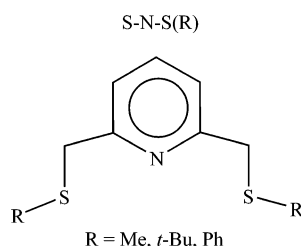
(5) (a) Ito, T. S.; Hasegawa, S.; Takahashi, Y.; Ishii, Y. *J. Organomet. Chem.* **1974**, 73, 401. (b) Susuki, H.; Itoh, K. Ishii, Y.; Simon, K.; Ibers J. A. *J. Am. Chem. Soc.* **1976**, 26, 8494.

Scheme 1

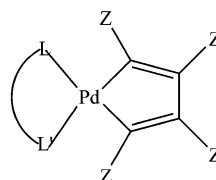
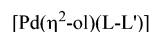
BIDENTATE LIGANDS



TERDENTATE LIGANDS



PALLADIUM COMPLEXES

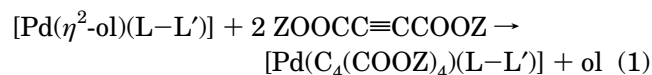


ol = tetramethylethylentetracarboxylate, maleic anhydride

L-L' = DPPQ-Me, TMQ-Me, RN-SR', S-N-S(R)

Z = COOMe, COOEt, COO*t*-Bu

On the basis of the well-established experience acquired in our laboratory about the steric and electronic characteristics of Pd(0) substrates carefully tuned by variously substituted bi- and terdentate pyridylthioethers and bearing different olefins⁶ we decided to undertake a detailed study on the reactivity of the complexes reported in Scheme 1 with respect to the cyclometalation induced by DMA according to reaction 1, with the awareness that no previous kinetic studies were carried out nor have mixed donor ligands been hitherto employed:



With the aim of clarifying the intimate mechanism governing this reaction and possibly establishing the conditions that allow the accumulation of a π -coordinated alkyne intermediate, we also studied reaction 1

with Pd(0) olefin complexes bearing phospho- and thioquinolines as mixed donor bidentate ligands.

Results and Discussion

General Considerations. Among all the Pd(0) olefin complexes studied in the present paper, only the DPPQ-Me and TMQ-Me derivatives represent novel substrates that have never been synthesized and described heretofore. Therefore, only the solution rearrangements of these species will be discussed, the characterization and the fluxional behavior of all other Pd(0) derivatives being widely dealt with elsewhere.^{6,7}

Pd(0) Olefin Complexes. The complexes $[\text{Pd}(\eta^2\text{-ol})(\text{DPPQ-Me})]$ (ol = tmetc, ma) and $[\text{Pd}(\eta^2\text{-tmetc})(\text{TMQ-Me})]$ were obtained by addition of the ancillary ligand (DPPQ-Me, TMQ-Me) and of the appropriate olefin to an anhydrous acetone solution of the precursor $\text{Pd}_2\text{DBA}_3\cdot\text{CHCl}_3$ under inert atmosphere (Ar). The formation of the complexes was monitored by means of ¹H and ¹³C NMR since the signals of the olefin and of the ancillary ligands shift upfield and downfield respectively upon coordination. In any case these complexes

(6) (a) Canovese, L.; Visentin, F.; Uguagliati, P.; Crociani, B. *J. Chem. Soc., Dalton Trans.* **1996**, 1921. (b) Chessa, G.; Canovese, L.; Visentin, F.; Uguagliati, P. *Inorg. Chem. Commun.* **1999**, 2, 607. (c) Canovese, L.; Visentin, F.; Chessa, G.; Uguagliati, P.; Dolmella, A. *J. Organomet. Chem.* **2000**, 601, 1. (d) Canovese, L.; Visentin, F.; Chessa, G.; Gardenal, G.; Uguagliati, P. *J. Organomet. Chem.* **2001**, 622, 155. (e) Canovese, L.; Chessa, G.; Santo, C.; Visentin, F.; Uguagliati, P. *Organometallics* **2002**, 21, 4342.

(7) Canovese, L.; Lucchini, V.; Santo, C.; Visentin, F.; Zambon, A. *J. Organomet. Chem.* **2002**, 642, 58.

behave differently in solution than their pyridylthioether analogues. The enhanced rigidity of the DPPQ-Me and TMQ-Me ancillary ligand skeleton with respect to the flexibly joined structure of pyridylthioethers hampers the apparent olefin rotation that is usually observed in the case of complexes bearing the latter as ancillary ligand. It is well known, in fact, that such a movement is principally due to rearrangement of the ancillary ligand (Pd–N or Pd–S cleavage and subsequent recombination) rather than to an effective olefin rotation, especially in the case of the tmtc moiety.^{6,7} The ¹H NMR analysis of the planar DPPQ-Me derivatives in the presence of an apparent olefin rotation would give rise to a symmetric spectrum for the olefin protons. At variance, the spectra clearly indicate the existence of a tightly coordinated olefin in an unsymmetrical environment. This situation may arise only from the presence of olefin protons (or substituents) lying *cis* or *trans* to phosphorus, as can be further deduced from the P–H and H–H coupling constants (see Experimental Section). The case of the complex [Pd(η^2 -tmetc)(TMQ-Me)] differs from those of the DPPQ-Me substrates. This complex, in fact, undergoes a fluxional rearrangement that could be interpreted on the basis of sulfur absolute configuration inversion. The olefin COOCH₃ protons yield a couple of singlets (3.73, 3.75 ppm) which do not collapse even at 183 K. In our experience this behavior can be traced back to the low-energy sulfur inversion process that is often operative even at the lowest temperature usually achievable.^{6,7}

Palladacyclopentadienyl Complexes. The palladacyclopentadienyl complexes were obtained under controlled atmosphere (Ar) by adding a slight excess of the polymeric precursor [Pd(C₄(COOZ)₄)]_n (Z = Me, Et, *t*-Bu) to a solution of the ligand L–L' in anhydrous acetone (see Scheme 1); the complexes [Pd(C₄(COOZ)₄)]_n (Z = Et, *t*-Bu) represent novel species that have never been synthesized so far. The same substrates could otherwise be obtained by reacting the Pd(0) olefin complex bearing the appropriate ancillary ligand L–L' with the activated alkyne ZC≡CZ (Z = Me, Et, *t*-Bu) in anhydrous CH₂Cl₂. In both cases the products were coincident, as shown by the superimposition of the ¹H, ¹³C NMR and IR spectra of the cyclopalladate species independently synthesized.

The palladacyclopentadienyl complexes, like their Pd(0) olefin precursors, undergo two coexisting different fluxional rearrangements, i.e., ancillary ligand rotation and sulfur absolute configuration inversion. The latter phenomenon, which represents the mechanism requiring less energy, can be easily revealed in the case of the pyridylthioether derivatives by means of the ¹H DNMR technique. As a matter of fact, the diastereotopic CH₂S protons at low temperature upon “freezing” of the sulfur inversion movement produce an AB system in the interval 3.5–4.5 ppm. The substituents R at sulfur and R' in position 6 of the pyridine ring play an important role in this respect. The R' group (R' = Me, Cl) induces distortion of the Pd–N bond with concomitant weakening of the bond itself, disfavoring sulfur inversion since the strengthening of the Pd–S bond as a synergic response occurs with consequent lowering of the sulfur inversion rate. An additional effect is generated by the R substituent at sulfur. As a matter of fact the stereo-

electronic characteristics of these groups influence the Pd–S bond, which can be strengthened when an electron-donor group increases the basicity of sulfur. Thus the rate of sulfur inversion as a function of the stereoelectronic characteristics of the substituent R follows the order Ph > Me > *t*-Bu independently of the nature of R'.

In the case of the complex [Pd(C₄(COOZ)₄)(TMQ-Me)], owing to the planarity of the metallacycle and the lack of an internal probe such as the methylene protons, no sulfur absolute configuration inversion is detected. This species however undergoes Pd–N (or Pd–S) bond cleavage and recombination analogously to its Pd(0) olefin complexes (vide supra). The rearrangement is clearly indicated by the appearance in the low-temperature (233 K) ¹H NMR spectrum of four distinct singlets in the interval 3.25–4.00 ppm ascribable to the COOCH₃ protons “frozen” to the right or to the left side and in near or in far position with respect to the palladium atom. At RT the two surviving observed singlets were assigned to the COOCH₃ protons lying near (broad singlet) or far (sharp singlet) from palladium (see Experimental Section). Similar behavior is noticed in the case of all the pyridylthioether derivatives that undergo similar fluxional rearrangements. The main difference among these substrates comes again from the presence of a substituent in position 6 of the pyridine ring (R' = Me, Cl). The already observed weakening of the Pd–N bond, in the case of the corresponding Pd(0) complexes, induces a considerable increase in the ligand fluxionality, thereby confirming the mechanistic picture proposed.^{6,7} In this case, presumably, the strengthened Pd–S bond acts as a pivot in the rearrangement process. Again, the sulfur substituents R play a secondary but noticeable role in the complexes bearing unsubstituted pyridine (R' = H); thus, an induced increase of sulfur basicity slows down the fluxional rearrangement.

The formation of complexes of the type [Pd(C₄(COOZ)₄)-(DPPQ-Me)] (Z = Me, Et, *t*-Bu) is duly confirmed by the ¹H and ³¹P NMR spectra since marked downfield shifts of the phosphorus ($\Delta\delta \geq 38$ ppm) and quinoline-CH₃ ($\Delta\delta \geq 0.32$ ppm) signals are detected upon coordination. At variance with the other Pd(II) cyclometalated complexes described above, no fluxional rearrangements at RT are observed for these substrates in their corresponding ¹H NMR spectra; thus, Z protons (Z = Me, Et, *t*-Bu) give rise to four distinguishable groups of signals in any case.

The palladacyclopentadienyl complexes bearing the potentially terdentate ligands S–N–S(R) (R = Me, *t*-Bu, Ph) were synthesized analogously to the other previously described species and identified by NMR technique. The RT ¹H NMR spectra of these substrates display only one broad singlet attributable to the CH₂-S protons (the signal of the S–N–S(*t*-Bu) derivatives being more broadened than those of the phenyl and methyl species). Moreover, the signals pertaining to the two sulfur substituents R are coincident irrespectively of their nature. The COOCH₃ protons resonate as two singlets attributable to the protons belonging to the groups near to or far from the palladium center, respectively. This strongly indicates the alternating coordination of the sulfur atoms lying on both wings of the potentially terdentate ligand. This rearrangement represents a quite usual phenomenon when terdentate

pyridylthioether ligands are used in palladium complexes bearing two coordination sites already occupied by nucleophiles.^{6e,8}

On decreasing the temperature, the signals attributable to COOCH₃ protons differentiate, showing in the case of the complex [Pd(C₄(COOMe)₄)(SNS(*t*-Bu))] at 213 K four separated singlets at 3.21, 3.58, 3.59, and 3.66 ppm, but only one S-C(CH₃)₃ signal at 1.22 ppm and only one AB system ascribable to endocyclic CH₂-S protons (integrating 4H) at 3.95 and 4.43 ppm (*J* = 14.6 Hz). No singlets (or other signals) belonging to the CH₂-S protons of the uncoordinated wing are detectable. Moreover, all the palladacyclopentadienyl SNS(R) complexes behave similarly since only small differences in temperature separate the phenomena in the case of differently substituted complexes. This behavior is not unprecedented, and in the case of the [PdCl(Me)(SNS(*t*-Bu))] derivative an analogous fluxionality was observed.^{8b} In this case, however, we suggest a rearrangement that takes into account a nitrogen-centered T-shaped intermediate.⁹ The pyridine nitrogen acting as a pivot in a roundabout movement allows the fast alternate coordination of the sulfur atoms. The cyclopentadienyl carbon *trans* to nitrogen never changes its position. Neither does the carbon *trans* to sulfur, the two interchanging rings being equivalent. The sulfur absolute configuration inversion does not happen since some sort of residual coordination is probably operative. An alternative explanation would take into account the formation of a symmetric pentacoordinate species bearing both sulfur substituents on the same side with respect to the complex main coordination plane and the cyclopentadienyl moiety perpendicular to the plane itself, which however evolves into an open structure upon precipitation at low temperature (*vide post*).

X-ray Crystal Structures. The molecular structures of the neutral complexes **1** ((2,6-bis(*tert*-butylthio)methyl)pyridine)(1,2,3,4-tetrakis(methoxycarbonyl)buta-1,3-diene-1,4-diyl)palladium ([Pd(C₄(COOMe)₄)(SNS(*t*-Bu))] and **2** ((2-((*tert*-butylthio)methyl)pyridine)(1,2,3,4-tetrakis(methoxycarbonyl)buta-1,3-diene-1,4-diyl)palladium ([Pd(C₄(COOMe)₄)(HNS(*t*-Bu))] together with the numbering scheme used, are shown as ORTEP¹⁰ drawings in Figures 1 and 2, respectively. Both complexes show the metal at the center of a distorted square planar environment. The distortion is toward a tetrahedral arrangement. However, for simplicity we will refer to the Pd main coordination plane as the basal or equatorial plane, although this is somewhat inadequate. In **1**, the atoms in the basal plane, other than Pd, are N, S(1), C(16), and C(19), and they deviate from the plane by 0.23, -0.22, 0.26, and -0.27 Å, respectively. In **2**, the set is made up by the atoms N, S, C(11), and C(14); they deviate from the equatorial plane by 0.16, -0.15, -0.18, and 0.17 Å, respectively. Also the Pd atoms lie off the main coordination plane, by 0.20 in **1** and 0.15 Å in **2**.

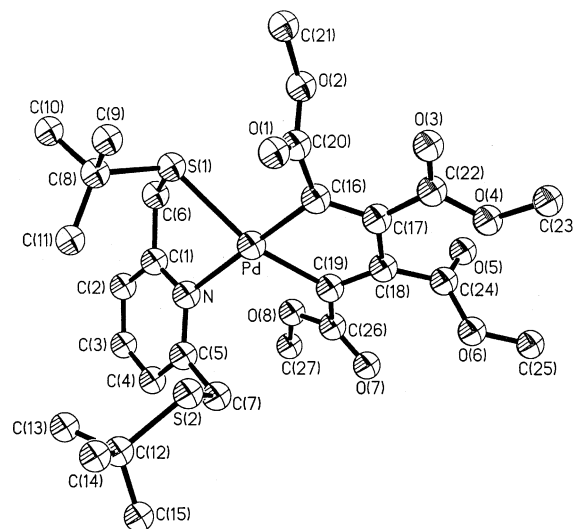


Figure 1. Molecular structure of complex **1**. Thermal ellipsoids are at the 40% probability level; hydrogen atoms have been omitted for clarity.

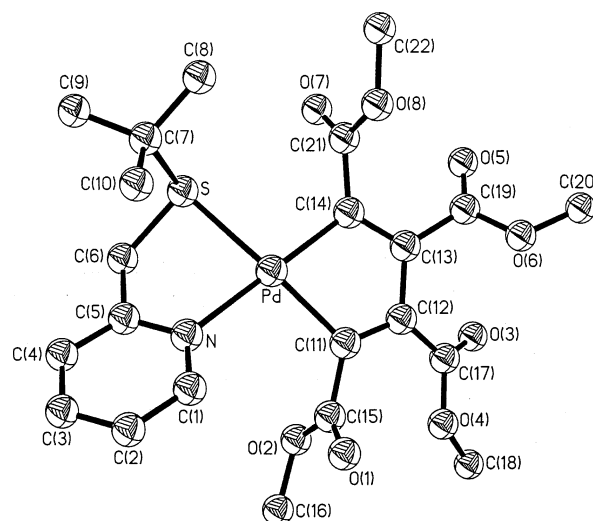


Figure 2. Molecular structure of complex **2**. The figure settings are as for **1**.

The above data indicate that **1** is more tetrahedrally distorted than **2**. The idea is confirmed by looking at the dihedral angle made by the triangles N-Pd-S(1) and C(16)-Pd-C(19) in **1** (24.8°) and by the triangles N-Pd-S and C(11)-Pd-C(14) in **2** (17.1°). Other indications are given by the departure of the angles S(1)-Pd-C(19) in **1** (156.0(1)°) and S-Pd-C(11) in **2** (163.0(1)°) from the ideal 180°, as well as by the deviation of the bite angles N-Pd-S(1) and C(16)-Pd-C(19) (81.9(1)° and 78.7(1)°) in **1** and N-Pd-S and C(11)-Pd-C(14) (82.9(1)° and 79.4(2)°) in **2** from the expected value of 90° for a regular square planar geometry.

The chelate ligands form, upon coordination, two five-membered rings in both **1** and **2**, whose overall main features are similar. In **1**, the atoms participating in the chelate pyridine ring, other than Pd, are N, C(1), C(6), and S(1); in **2**, the corresponding atoms are N, C(5), C(6), and S. In both complexes this ring assumes a *twist-envelope* (half-chair, C₂) arrangement, with the sulfur atom "at the flap", outside the mean plane defined by the remaining four atoms. In **1**, the atoms in this plane

(8) (a) Canovese, L.; Visentin, F.; Uguagliati, P.; Lucchini, V.; Bandoli, G. *Inorg. Chim. Acta* **1998**, *277*, 247. (b) Canovese, L.; Visentin, F.; Chessa, G.; Uguagliati, P.; Santo, C.; Bandoli, G.; Maini, L. *Organometallics* **2003**, *22*, 3230.

(9) (a) Thorn, D. L.; Hoffmann, R. *J. Am. Chem. Soc.* **1978**, *100*, 2079. (b) Gogoll, A.; Örnebro, J.; Grennberg, H.; Bäckwall, J. *J. Am. Chem. Soc.* **1994**, *116*, 3632. (c) Albinati, A.; Kunz, R. W.; Ammann, C. J.; Pregosin, P. S. *Organometallics* **1991**, *10*, 1800.

(10) Johnson, C. K. *ORTEP*, Report ORNL-5138; Oak Ridge National Laboratory: Oak Ridge, TN, 1976.

deviate up to 0.07 Å, with the sulfur off by 1.00 Å; in **2**, the atoms deviate up to 0.02 Å, with the sulfur off by 0.86 Å. The five-membered ring planes Pd–N–C(1)–C(6)–S(1) (in **1**) and Pd–N–C(5)–C(6)–S (in **2**) make dihedral angles of 26.9° and 20.5°, respectively, with the main coordination plane. As for the ring formed by the butadienyl ligand, the atoms participating in it, besides the metal center, are C(16), C(17), C(18), C(19) and C(11), C(12), C(13), C(14) in **1** and **2**, respectively. In both complexes these rings are virtually planar, with deviations from the mean ring plane limited to 0.03 Å in **1** and 0.05 Å in **2**. In complex **1**, the plane of this ring makes dihedral angles of 14.7° and 39.1° with the basal plane and the Pd–N–C(1)–C(6)–S(1) plane, respectively. In complex **2**, the corresponding angles are 11.4° and 31.1°.

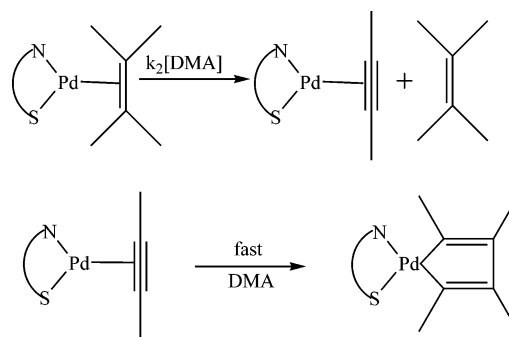
The orientation of the four C–C(=O)–OCH₃ residues in the butadienyl ligand of the two complexes also deserves some comments. In **1**, the residues I–IV branch from C(16), C(17), C(18), and C(19), respectively, and define angles of 91.4°, 14.3°, 99.8°, and 31.0°, respectively, with the main coordination plane. The reciprocal orientation of the residues is such that the mean plane of residue II is nearly orthogonal to those of residue I (89.5°) and III (87.9°). In **2**, the residues I–IV branch from C(11), C(12), C(13), and C(14), respectively, and define angles of 74.7°, 37.2°, 26.1°, and 72.8°, respectively, with the basal plane. As for their reciprocal orientation, the mean plane of residue IV is roughly perpendicular to that of residue II (71.9°) and almost coplanar to that of residue I (18.1°).

With respect to bond distances, they look similar overall in **1** and **2**. The Pd–S distance in **1** (2.394(1) Å) is ca. 0.02 Å longer than in **2** (2.369(1) Å), whereas the Pd–N distances are alike (2.126(2) and 2.126(4) Å in **1** and **2**, respectively). On the contrary, both molecules show one Pd–C distance shorter than the other (1.997(3), 2.040(2) Å in **1** and 2.013(4), 2.042(4) Å in **2**). The shortest distance is always the one where the σ -bonded carbon is *trans* to nitrogen; besides, the shortest Pd–C distance in **1** is also ca. 0.02 Å shorter than the shortest Pd–C distance in **2**.

To compare our data with those already published, we performed a search in the Cambridge Crystallographic Database¹¹ looking for mononuclear, neutral square planar Pd(II) complexes showing the N_{pyr}–S–C–C/Cl donor set (N_{pyr} = pyridine nitrogen). The search returned seven structures.^{12–16}

A comparison with the present results as well as with other results from our group is feasible.¹⁷ To the best of our knowledge, **1** and **2** are the first reported

Scheme 2



examples of mononuclear neutral square planar Pd(II) complexes showing the N_{pyr}–S–C–C donor set.

Data indicate that the Pd–S bond distances in **1** and **2** are the longest in this group of molecules. This is due, in our opinion, to the stronger *trans* influence of the negatively charged C σ -bonded ligand over the sulfur donor. In fact, in the other molecules examined the sulfur donor is faced either by a pyridine nitrogen^{12–14} or by a chloride,^{15–17} both of them softer bases. In **1** and **2** also the pyridine nitrogen atom is faced by a negatively charged σ -bonded C ligand. Thus, the Pd–N distances are longer than those found in the complexes where the nitrogen is *trans* to sulfur (a softer base),^{12–14} yet shorter than those found in the other known complexes where the nitrogen is *trans* to a negatively charged C atom.^{16,17} The Pd–C distances (see above) show a dual behavior. In fact, the shortest Pd–C distances in **1** and **2** are similar to those found in the other complexes where the σ -bonded C ligand belongs to an olefin moiety,^{12–14,17} whereas the longest Pd–C bonds are similar to those found in the complexes where the C donor atom belongs to a methide group.^{15,16}

Kinetic and Mechanistic Study. The oxidative coupling of DMA promoted by the [Pd(η^2 -ol)(RN-SR')] derivatives (ol = ma, tmetc; R = H, Cl; R' = Me, Ph, *t*-Bu) was studied by ¹H NMR technique or by UV/vis spectrophotometry under pseudo-first-order conditions. In this respect, to 3 mL of prethermostated solution of the complex under study ([Pd]₀ = 10^{−4} mol dm^{−3} in freshly distilled CHCl₃) was added a microaliquot of DMA solution ([DMA]₀ ≥ 20[Pd]₀). In the literature, some qualitative studies were carried out using ma derivatives,^{5a} unfortunately in our case the ma complexes upon DMA addition give rise to a very fast reaction leading to the cyclopalladate species. Conversely, when tmetc derivatives are studied, the absorbance change associated with the reaction in Scheme 2 is generally described by the following monoexponential expression:

$$A_t = A_\infty + (A_0 - A_\infty)e^{-k_{\text{obs}}t} \quad (2)$$

where A_t , A_∞ , and A_0 represent the absorbance of the reaction mixture at time t , at the end, and at the beginning of the reaction, k_{obs} being the observed pseudo-first-order rate constant. In this respect the use of this home-synthesized bulky olefin slows the reaction rate, allowing a detailed study of the oxidative DMA coupling on Pd(0) substrates. Linear regression of the ensuing k_{obs} vs alkyne concentration for each complex gives rise to the second-order rate constants listed in Table 1.

(11) Allen, F. H. *Acta Crystallogr.* **2002**, B58, 380; Cambridge Structural Database (Version 5.25 of November 2003 + 3 updates).

(12) Spencer, J.; Pfeffer, M.; DeCian, A.; Fischer, J. *J. Org. Chem.* **1995**, 60, 1005 (entry code SUPMIZ).

(13) Spencer, J.; Pfeffer, M.; Kyritsakas, N.; Fischer, J. *Organometallics* **1995**, 14, 2214 (entry codes ZAF CUE, ZAF DEF).

(14) Dupont, J.; Basso, N. R.; Meneghetti, M. R.; Konrath, R. A.; Burrow, R.; Horner, M. *Organometallics* **1997**, 16, 2386 (entry code RUQVOO).

(15) Canovese, L.; Visentin, F.; Chessa, G.; Uguagliati, P.; Bandoli, G. *Organometallics* **2000**, 19, 1461 (entry codes XEKVAK, XEKVEO).

(16) Canovese, L.; Visentin, F.; Chessa, G.; Santo, C.; Uguagliati, P.; Bandoli, G. *J. Organomet. Chem.* **2002**, 650, 43 (entry code HUGGAR).

(17) Canovese, L.; Visentin, F.; Chessa, G.; Uguagliati, P.; Santo, C.; Dolmella, A. *Organometallics* **2005**, 24, 3297.

Table 1. Second-Order Rate Constants ($\text{mol}^{-1} \text{dm}^3 \text{s}^{-1}$) for the Reaction of the Complex $[\text{Pd}(\eta^2\text{-tmetc})(\text{RN-SR}')] \text{ with DMA in } \text{CHCl}_3 \text{ at } 25^\circ \text{C}$

	R = H	R = Me	R = Cl
R' = Me	0.20 ± 0.02	0.09 ± 0.02	10.5 ± 0.5
R' = Ph	0.137 ± 0.005	0.114 ± 0.005	10.8 ± 0.5
R' = <i>t</i> -Bu	0.015 ± 0.001		2.59 ± 0.05

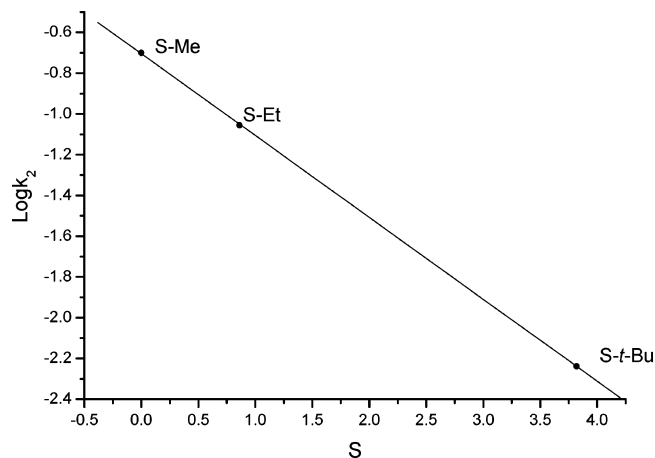
Table 2. Second-Order Rate Constants ($\text{mol}^{-1} \text{dm}^3 \text{s}^{-1}$) for the Reaction of the Complex $[\text{Pd}(\eta^2\text{-tmetc})(\text{HN-SMe})] \text{ with } \text{ZC}\equiv\text{CZ} \text{ in } \text{CHCl}_3 \text{ at } 25^\circ \text{C}$

Z = COOMe	Z = COOEt	Z = COO <i>t</i> -Bu
0.199 ± 0.002	0.088 ± 0.002	0.006 ± 0.001

The monoexponential absorbance change, the failure to observe any intermediate (^1H NMR check), and the linear dependence of k_{obs} on the concentration of the alkyne suggest a steady state mechanism in which a reactive Pd(0) monoalkyne intermediate species reacts immediately to give the reaction product. In this respect, the second-order rate constants experimentally determined are referred to the first alkyne-dependent rate-determining stage (Scheme 2). This reaction profile is also maintained if the bulkiness of the ester group Z on the alkyne moiety is increased. In Table 2 the second-order rate constants as a function of the alkyne substituent Z group are reported in the case of the complex $[\text{Pd}(\eta^2\text{-tmetc})(\text{HN-SMe})]$.

The associative nature of the first alkyne attack is confirmed by the correlation of $\log k_2$ vs the front strain steric parameter S^{18} (Figure 3) and by the activation parameters determined by the reparametrized Eyring plot¹⁹ for the same complex reacting with DMA in the temperature range 288–313 K. The ensuing activation parameters are $\Delta H^\ddagger = 13 \pm 2 \text{ kJ mol}^{-1}$ and $\Delta S^\ddagger = -19 \pm 7 \text{ J mol}^{-1} \text{ K}^{-1}$. These values are in line with those found in associative olefin exchange reactions among Pd(0) derivatives bearing pyridylthioether ligands.⁶

From the data in Tables 1 and 2, the lowering of the rate constants on increasing the steric demand of the ancillary ligand and entering alkyne is evident. However, it might be noticed that the substituents R on the pyridine ring affect the reaction rates to a different extent, and thus the ensuing reactivity cannot be easily traced back to the substituent bulkiness. As a matter of fact, the reactivity hardly changes on going from complexes bearing R' = H to those with R' = Me (a similar conclusion is drawn when the Pd(0) pyridylthioether olefin substrates are compared in olefin exchange reactions, since also in these reactions the pyridine substituent (H vs Me) hardly affects the overall reactivity^{6c-e}). Conversely, it has been shown¹⁵⁻¹⁷ that distortion due to the pyridine substituent (R' = Me, Cl) strongly influences the reactivity toward insertion of unsaturated molecules in Pd(II) pyridylthioether derivatives, chlorine being the most effective for electronic reasons. In the present case, as can be seen in Table 1, the presence of a chlorine group in position 6 of the pyridine ring, having a hindrance analogous to that of the methyl group, imparts a reactivity enhanced by about 2 orders of magnitude to the corresponding

**Figure 3.** Plot of $\log k_2$ vs front strain parameters (ref 17).

derivatives. This remarkable behavior is probably the net result between an unfavorable steric hindrance and an overwhelming tendency to chelate ring opening due to a lowered basicity of the chlorine-substituted pyridine. This will provide for an easier entry of the first alkyne into the coordination sphere of the transition state carrying the bulky leaving olefin and the incoming alkyne simultaneously bound to palladium.

For the sake of completeness the reactivity of substrates bearing a rigid ancillary ligand was investigated, and in this respect $[\text{Pd}(\eta^2\text{-tmetc})(\text{TMQ-Me})]$ reacts slowly with DMA (rate constant = $0.052 \pm 0.001 \text{ mol}^{-1} \text{dm}^3 \text{s}^{-1}$). Since the complex $[\text{Pd}(\eta^2\text{-tmetc})(\text{TMQ-Me})]$ is moderately less reactive than $[\text{Pd}(\eta^2\text{-tmetc})(\text{MeN-SMe})]$, one might advance the hypothesis that rigidity of the TMQ-Me ligand skeleton disfavors the crowded transition state determined by the incoming DMA. It is moreover noteworthy that the exchange of a sulfur donor with phosphorus renders the corresponding $[\text{Pd}(\eta^2\text{-tmetc})(\text{DPPQ-Me})]$ complex almost unreactive.

A further indication about the associative nature of the first alkyne attack is represented by the high reaction rates found in the case of complexes bearing scarcely hindered olefins. The complexes $[\text{Pd}(\eta^2\text{-ma})(\text{R}'\text{N-SR})]$ (R' = H, Me, Cl; R = Me, Ph) indeed react immediately with DMA, and in this respect the associative alkyne attack is in line with previous findings on olefin exchange reactions that were extensively studied so far.⁶

Complexes with MeN-*St*-Bu as Ancillary Ligand.

Apparently the monoalkyne intermediate is a very reactive species. It is however known that similar monoalkyne species could be stabilized and obtained by increasing the π -acidity^{5a} and/or the bulkiness of the ancillary ligand.²⁰ In this respect we chose to study the kinetics of addition of DMA to the complex $[\text{Pd}(\eta^2\text{-tmetc})(\text{MeN-}i\text{St-Bu})]$ in the hope of isolating the monoalkyne intermediate or alternatively to gain further information on its mechanistic behavior. As expected, the spectral absorbance changes detected by UV/vis technique do not obey a monoexponential law, the trend rather suggesting a buildup of an intermediate. Accordingly, analysis of the related ^1H NMR spectra (see Figure 4) shows the accumulation of an intermediate

(18) Beckhaus, H.-D. *Angew. Chem., Int. Ed. Engl.* **1978**, *17*, 593.(19) Uguagliati, P.; Michelin, R. A.; Belluco, U.; Ros, R. *J. Organomet. Chem.* **1979**, *169*, 115.(20) tom Dieck, H.; Munz, C.; Müller, C. *J. Organomet. Chem.* **1990**, *384*, 243.

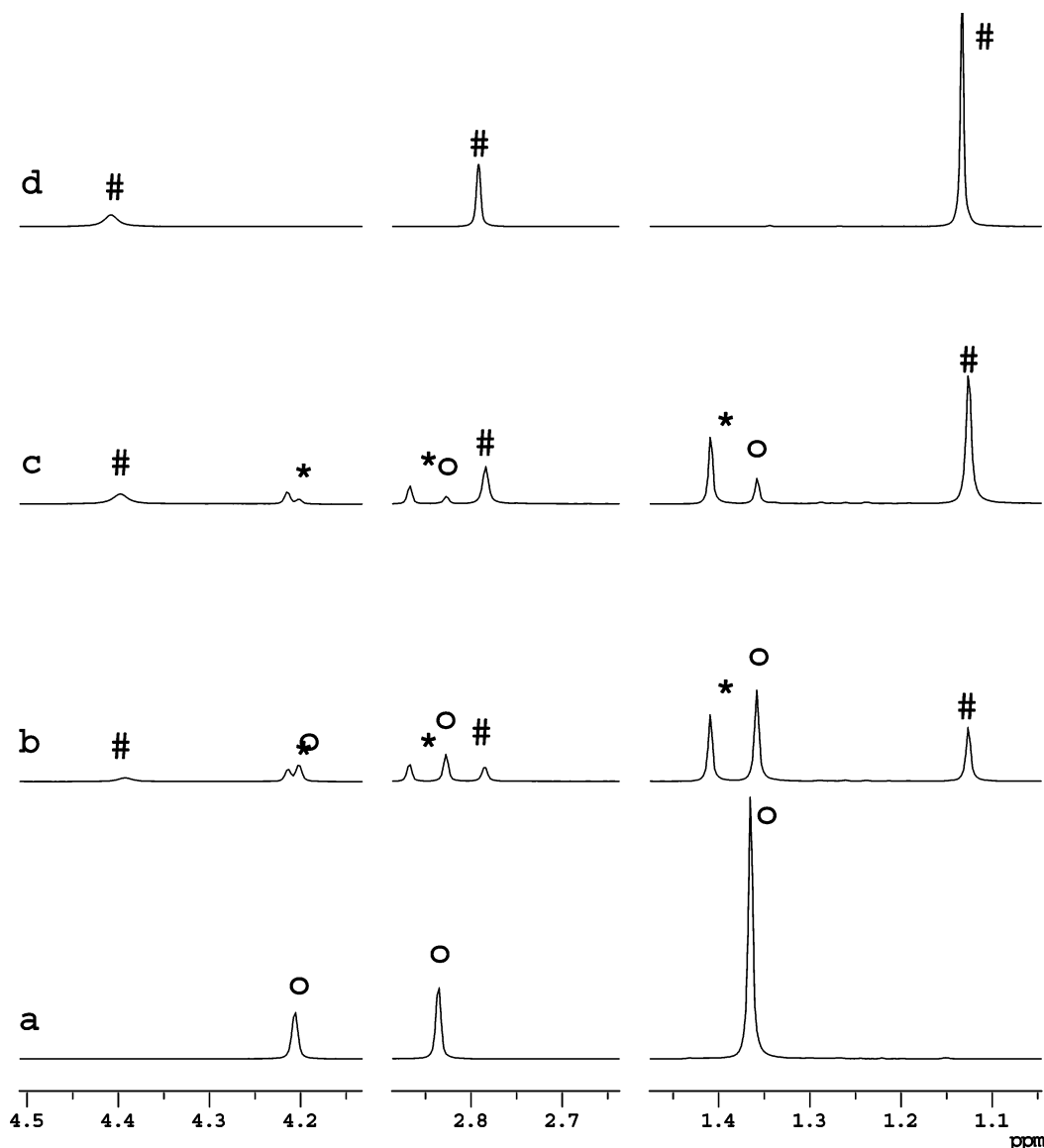


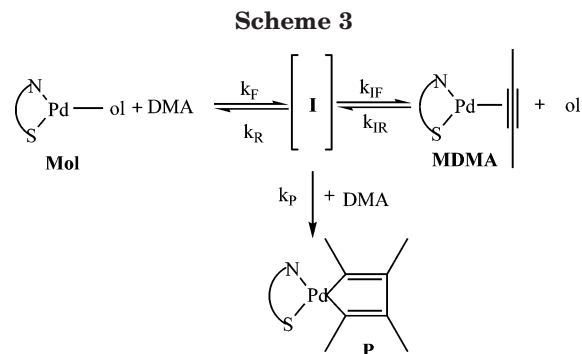
Figure 4. Time-dependent ^1H NMR spectra for the reaction between $[\text{Pd}(\eta^2\text{-tmetc})(\text{MeN-St-Bu})]$ and DMA: (a) spectrum of an authentic sample of $[\text{Pd}(\eta^2\text{-tmetc})(\text{MeN-St-Bu})]$, $t = 0$; (b) $t = 8$ min after DMA addition; $t = 26$ min after DMA addition; (d) spectrum of an authentic sample of $[\text{Pd}(\text{C}_4(\text{COOMe})_4)(\text{MeN-St-Bu})]$. # = $[\text{Pd}(\eta^2\text{-DMA})(\text{MeN-St-Bu})]$.

species characterized by the signals pertaining to a pyridine ring very near to those of the starting substrate in the interval 7.15–7.75 ppm. Signals ascribable to $\text{CH}_2\text{-S}$, Pyr-CH_3 , and $\text{C}(\text{CH}_3)_3$ were also detected as one broad and two sharp singlets at 4.22, 2.87, and 1.41 ppm, respectively. The time-dependent concentration of this species can be described by the unsymmetrical bell-shaped profile typical of an intermediate species. Moreover the amount of free tmetc olefin matches with the sum of the concentrations of the intermediate and the final compounds. No coordinated DMA is however detected since its signal falls in a very crowded spectral region, and moreover, similarly to the analogous Pd(0) olefin derivatives, this complex undergoes fast exchange between the coordinated and the uncoordinated unsaturated moiety.

The analysis of concentration profiles does not allow a simple interpretation. The simple model based on a slow equilibrium reaction giving rise to a monoalkyne intermediate followed by an irreversible reaction does not fit the ^1H NMR experimentally detected concentra-

tion changes of the starting, the intermediate, and the final cyclopalladate product. On the other hand, the plausible model involving two slow equilibria was ruled out because the cyclopalladate complex is unreactive even in the presence of a large excess of tmetc. Careful analysis of the spectra suggests that the monoalkyne compound represents in this case the quite stable product of an alternative route rather than a reactive intermediate. As a matter of fact, its accumulation is favored by the steric hindrance of the ancillary ligand, which prevents to some extent the attack of the free alkyne. Thus, the cyclopalladate becomes the result of the multistep mechanism shown in Scheme 3, in which a simplified reaction path used as a mechanistic model is reported. The undetected reactive intermediate **I** is likely to be a mixed olefin-alkyne Pd(0) species.

The fit of the time-dependent concentrations recorded from ^1H NMR data to time according to the proposed mechanism is shown in the Figure 5. The fit of the concentration profiles for this complex system, while being fairly good, is affected by high parameter correla-



tion coefficients, which are reflected by high standard errors of estimates for the fitted parameters. Nevertheless, it is noteworthy that the fitted k_F value ($0.024 \pm 0.001 \text{ mol}^{-1} \text{ dm}^3 \text{ s}^{-1}$), which is the most accurately determined parameter, is in substantial accord with the second-order rate constants reported in Table 1.

The reaction between the complex $[\text{Pd}(\eta^2\text{-ma})(\text{MeN-}i\text{StBu})]$ and DMA would induce the accumulation of the monoalkyne intermediate irrespectively of the leaving olefin, since only the bulkiness of the $\text{MeN-}i\text{StBu}$ ligand forces the reaction toward the production of such derivative. The ^1H NMR experiment unequivocally shows indirectly the accumulation of the intermediate. As a matter of fact, the free ma, which is detected as a broad singlet at ≈ 7 ppm, originated by displacement from the $[\text{Pd}(\eta^2\text{-ma})(\text{MeN-}i\text{StBu})]$ complex by the alkyne attack at the beginning of the reaction, is in large excess with respect to the final cyclopalladate product, which is present in traces. This is a strong indication of the fast accumulation of an intermediate which subsequently reacts slowly to give the product. The intermediate is not detected since free ma exchanges rapidly with the alkyne of the monocoordinated alkyne intermediate. The free ma also exchanges with the coordinated olefin of the starting complex, as can be seen by the small shifts and the general broadening of all the signals. The equilibrium constant K_E related to the displacement of ma by DMA was estimated by NMR and confirmed by spectrophotometric titration ($K_E = 0.0140 \pm 0.003$). Figure 6 reports the absorbance data vs the concentration of the titrant DMA and the corresponding fit. Pd(0) gives rise with ma to more stable complexes than those bearing tmetc. However, owing to its reduced steric hindrance, ma itself is rapidly displaced by the entering unsaturated moiety. This result parallels those found in the former studies dealing with olefin exchanges in Pd(0) olefin derivatives.⁶

The fast formation of the intermediate does not allow fast formation of the cyclopalladate product since the rate of reaction is lowered by the formation of the same scarcely reactive monoalkyne derivative obtained in the case of $[\text{Pd}(\eta^2\text{-tmetc})(\text{MeN-}i\text{StBu})]$. Moreover, the very small absorbance change associated with product formation hampers any attempt at precise determination of the kinetic constants by spectrophotometric technique under pre-equilibrium conditions.

Formation of Hexamethylmellitite. The NMR spectra obtained under mild experimental conditions and at low DMA/complex ratios show the formation of hexamethylmellitite as a side product of the quantitative production of cyclopalladate. Such a symmetric compound was identified from its characteristic singlet

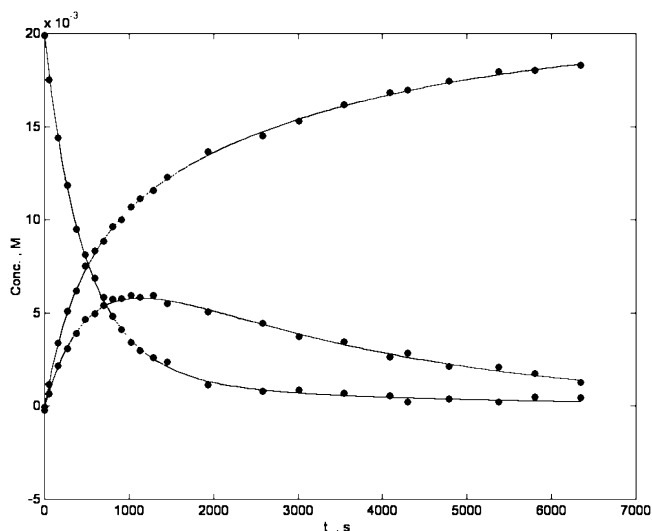


Figure 5. Fit of NMR-determined concentration profiles according to the mechanism in Scheme 3.

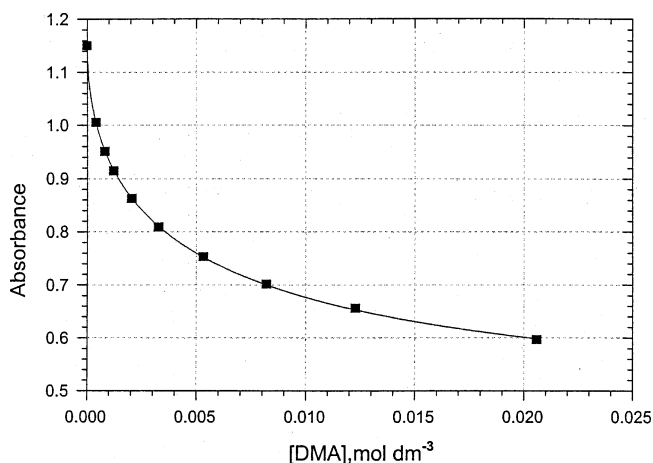


Figure 6. Spectrophotometric determination of equilibrium constant K_E for the reaction of $[\text{Pd}(\eta^2\text{-ma})(\text{MeN-}i\text{StBu})]$ with DMA in CHCl_3 at 25°C . Fit of absorbance vs $[\text{DMA}]$ at $\lambda = 287 \text{ nm}$.

at 3.87 ppm in CDCl_3 , separated after complete precipitation of the cyclometalate complexes from the mother liquor by HPLC and characterized by mass spectrometry. Its mechanism of formation appears to be rather complicated, since, contrary to our expectation, the stable cyclopalladate substrate does not react with one further alkyne molecule to give the mellitite under mild conditions.

Moreover, preliminary investigation shows that mellitite production is not monotonically dependent on alkyne concentration. Since the palladium-mediated synthesis of this species usually requires long time, high temperature, and high alkyne excess,^{4c} we intend to investigate exhaustively its mechanism of formation in a forthcoming study.

Experimental Section

Solvents and Reagents. Acetone and CH_2Cl_2 were distilled over CaH_2 and 4 Å molecular sieves, respectively, under inert atmosphere (Ar). Chloroform was distilled and stored over silver foil. All the other chemicals were commercially available grade products unless otherwise stated.

IR, NMR, and UV-Vis Measurements. The IR and ^1H and $^{13}\text{C}\{^1\text{H}\}$ NMR spectra were recorded on a Perkin-Elmer Spectrum One spectrophotometer and on a Bruker 300 Avance spectrometer, respectively. The proton and carbon assignment was performed by ^1H - ^{13}C -HMQC and -HMBC experiments. UV-vis spectra were taken on a Perkin-Elmer Lambda 40 spectrophotometer equipped with a Perkin-Elmer PTP6 (Peltier temperature programmer) apparatus.

X-ray Diffraction Analysis. Crystals of **1** and **2** suitable for X-ray analysis were mounted on the top of a glass fiber, coated with epoxy resin, and placed on the goniometer head of a STADI 4 CCD diffractometer. Data were collected at room temperature using graphite-monochromated Mo K α radiation ($\lambda = 0.71073 \text{ \AA}$) and corrected for Lorentz and polarization effects as well as for absorption.

The two structures were solved by the heavy-atom methods using the SHELXTL NT²¹ computer program and refined on F^2 by standard full-matrix least-squares with SHELXL-97.²² All non-hydrogen atoms were refined anisotropically; the hydrogen atoms were placed in calculated positions and refined as a riding model. A summary of crystal and refinement data is reported in Table 1Si; Table 2Si lists selected bond distances and angles of the two complexes.

Preliminary Studies and Kinetic Measurements. All the cycloaddition reactions were preliminarily analyzed by ^1H NMR technique by dissolving the complex under study in 0.6 mL of CDCl_3 ($[\text{complex}]_0 \approx 2 \times 10^{-2} \text{ mol dm}^{-3}$). An appropriate aliquot of alkyne was added ($[\text{alkyne}]_0 \approx 4.1 \times 10^{-2} \text{ mol dm}^{-3}$), and the reaction was followed to completion by monitoring the signals for the disappearance of the starting complex and the contemporary appearance of the cyclopalladate species.

A UV-vis preliminary investigation was also performed with the aim of determining a suitable wavelength. For this purpose, 3 mL of freshly distilled CHCl_3 solution of the complex under study ($[\text{complex}]_0 \approx 1 \times 10^{-4} \text{ mol dm}^{-3}$) was placed in a thermostated (25 °C) cell compartment of the UV-vis spectrophotometer, and microaliquots of a concentrated solution of the alkyne were added. The absorbance change was monitored in the 245–500 nm wavelength interval.

Synthesis of the Bidentate and Terdentate Ligands. The synthesis of the ligands 6-chloro-2-*tert*-butylthiomethylpyridine (CIN-*St*-Bu), 6-chloro-2-phenylthiomethylpyridine (CIN-SPh), 6-chloro-2-methylthiomethylpyridine (CIN-SMe),¹⁵ 6-methyl-2-phenylthiomethylpyridine (MeN-SPh), 6-methyl-2-*tert*-butylthiomethylpyridine (MeN-*St*-Bu), 2-phenylthiomethylpyridine (HN-SPh), 2-*tert*-butylthiomethylpyridine (HN-*St*-Bu),²³ 2-methylthiomethylpyridine (HN-SMe),^{6c} 6-methyl-2-methylthiomethylpyridine (MeN-SMe),²⁴ 2,6-bis(phenylthiomethyl)pyridine (S-N-S(Ph)), 2,6-bis(*tert*-butylthiomethyl)pyridine (S-N-S(*t*-Bu)),^{6d} 2,6-bis(methylthiomethyl)pyridine (S-N-S(Me)),²⁵ and 8-diphenylphosphanyl-2-methylquinoline (DPPQ-Me)¹⁶ was carried out according to published procedures. All other chemicals were commercial grade and were purified or dried by standard methods where required.²⁶

2-Methyl-8-thiomethylquinoline (TMQ-Me). To 1.01 g (18.1 mmol) of KOH in 20 mL of anhydrous DMSO were added 3.156 g (45.03 mmol) of CH_3SNa and 2 g (9 mmol) of 8-bromoquinoline. The resulting mixture was stirred under inert atmosphere (N_2) for 5 h at RT and overnight at 80 °C.

(21) Sheldrick, G. M. *SHELXTL NT*, Version 5.10; Bruker AXS Inc.: Madison, WI, 1999.

(22) Sheldrick, G. M. *SHELXL-97*, Program for the Refinement of Crystal Structures; University of Göttingen: Göttingen, Germany, 1997.

(23) Canovesi, L.; Visentin, F.; Uguagliati, P.; Chessa, G.; Pesce, A. *J. Organomet. Chem.* **1998**, *566*, 61.

(24) Canovesi, L.; Chessa, G.; Santo, C.; Visentin, F.; Uguagliati, P. *Inorg. Chim. Acta* **2003**, *346*, 158.

(25) Canovesi, L.; Chessa, G.; Marangoni, G.; Pitteri, B.; Uguagliati, P.; Visentin, F. *Inorg. Chim. Acta* **1991**, *186*, 79.

(26) Armarego, W. L. F.; Perrin, D. D. In *Purification of Laboratory Chemicals*, 3rd ed.; Pergamon: New York, 1988.

Water (50 mL) was then added, and the reaction products were extracted by Et_2O (50 mL). The organic solution was dried over MgSO_4 (6 h), filtered, and dried under vacuum. The purification of the crude product was achieved by flash chromatography through a silica column with CH_2Cl_2 as eluent. Concentration under vacuum of the eluate yields 1.005 g (5.3 mmol) of the pale yellow compound. Yield: 59% IR (KBr pellet): $\nu_{\text{C}=\text{N}}$ 1564.9 cm^{-1} . ^1H NMR (CDCl_3 , $T = 298 \text{ K}$, ppm): thiomethyl protons, δ , 2.58 (s, 3H, S- CH_3), methyl protons 2.79 (s, 3H, Qui- CH_3), quinoline protons 7.32 (d, 1H, H^3_{qui} , $J = 8.4 \text{ Hz}$), 7.37 (dd, 1H, H^7_{qui} , $J = 7.3$; 1.5 Hz), 7.44 (t, 1H, H^6_{qui} , $J = 7.6 \text{ Hz}$), 7.53 (dd, 1H, H^5_{qui} , $J = 7.9$; 1.5 Hz), 8.02 (d, 1H, H^4_{qui} , $J = 8.4 \text{ Hz}$). ^{13}C NMR (CDCl_3 , $T = 298 \text{ K}$, ppm): quinoline carbons, δ , 158.6 (C^2_{qui}), 122.9 (C^3_{qui}), 136.6 (C^4_{qui}), 126.3 (C^5_{qui}), 126.1 (C^6_{qui}), 123.0 (C^7_{qui}), 139.5 (C^8_{qui}), 145.4 (C^9_{qui}), 126.5 ($\text{C}^{10}_{\text{qui}}$), thiomethyl carbons 14.6 (qui-S- CH_3), methyl carbons 25.8 (qui- CH_3).

Synthesis of Pd(0) Olefin Complexes Bearing Bidentate Ligands. [Pd(η^2 -tmetc)(TMQ-Me)]. 2-Methylthiomethylquinoline (TMQ-Me, 0.058 g, 0.345 mmol), 0.0792 g (0.345 mmol) of tmetc, and 0.150 g (0.145 mmol) of $\text{Pd}_2\text{DBA}_3 \cdot \text{CHCl}_3$ were dissolved under inert atmosphere (N_2) in 15 mL of anhydrous acetone. The resulting solution was stirred for 1 h, treated with activated charcoal, and eventually filtered off on a Celite filter. Concentration under reduced pressure and addition of Et_2O yields 0.142 g (0.25 mmol) of the title product as pale yellow microcrystals. Yield: 88%. IR (KBr pellet): $\nu_{\text{C}=\text{O}}$ 1703.1, $\nu_{\text{C}=\text{N}}$ 1564.9 cm^{-1} . ^1H NMR (CDCl_3 , $T = 298 \text{ K}$, ppm): thiomethyl protons, δ , 2.90 (s, 3H, S- CH_3), methyl protons 3.14 (s, 3H, CH_3 -qui), ester protons 3.73 (s, 6H, COOCH_3), 3.75 (s, 6H, COOCH_3), quinoline protons 7.53 (d, 1H, H^3_{qui} , $J = 8.5 \text{ Hz}$), 7.57 (t, 1H, H^6_{qui} , $J = 7.3 \text{ Hz}$), 7.83 (dd, 1H, H^5_{qui} , $J = 8.0$; 1.2 Hz), δ 7.99 (dd, 1H, H^7_{qui} , $J = 7.3$; 1.4 Hz), δ 8.2 (d, 1H, H^4_{qui} , $J = 8.5 \text{ Hz}$). ^{13}C NMR (CDCl_3 , $T = 298 \text{ K}$, ppm): quinoline carbons, δ , 165.26 (C^2_{qui}), 124.29 (C^3_{qui}), 138.96 (C^4_{qui}), 129.68 (C^5_{qui}), 126.77 (C^6_{qui}), 135.33 (C^7_{qui}), 134.84 (C^8_{qui}), 148.26 (C^9_{qui}), 128.45 ($\text{C}^{10}_{\text{qui}}$), thiomethyl carbons 25.88 (qui-S- CH_3), methyl carbons 31.00 (qui- CH_3), 52.54–52.77 (OCH_3), vinyl carbons 89.02–89.96 ($\text{C}=\text{C}$), carbonyl carbons 170.19–170.40 ($\text{C}=\text{O}$). Anal. Calcd for $\text{C}_{23}\text{H}_{29}\text{NO}_8\text{PdS}$: C 47.14, H 4.99, N 2.39. Found: C 47.31, H 4.92, N 2.42.

The following complexes were synthesized in an analogous way using the appropriate ligand and olefin.

[Pd(η^2 -tmetc)(CIN-SPh)]. Yield: 83% (pale yellow microcrystals). IR (KBr pellet): $\nu_{\text{C}=\text{O}}$ 1703.1, $\nu_{\text{C}=\text{N}}$ 1564.9 cm^{-1} . ^1H NMR (CDCl_3 , $T = 298 \text{ K}$, ppm): methyl ester protons, δ , 3.64 (s, 12H, COOCH_3), thiomethyl protons 4.51 (s, 2H, Pyr- CH_2S), pyridine protons 7.20 (d, 1H, H^5_{pyr} , $J = 7.6 \text{ Hz}$), 7.41 (d, 1H, H^3_{pyr} , $J = 7.6 \text{ Hz}$), 7.64 (t, 1H, H^4_{pyr} , $J = 7.7 \text{ Hz}$), phenyl protons 7.26–7.39 (bm, 3H, H_{ortho} , H_{para}), 7.43 (bm, 2H, 2H_{meta}). ^{13}C NMR (CDCl_3 , $T = 298 \text{ K}$, ppm): pyridine carbons, δ , 158.73 (C^2_{pyr}), 121.97 (C^3_{pyr}), 140.04 (C^4_{pyr}), 124.85 (C^5_{pyr}), thiomethyl carbon 47.44 (Pyr- CH_2S), methyl carbons 47.44 (COOCH_3), phenyl carbons 129.76 (C_{ortho}), 132.90 (C_{meta}), 129.41 (C_{para}), carbonyl carbons 169.89 ($\text{C}=\text{O}$). Anal. Calcd for $\text{C}_{22}\text{H}_{23}\text{ClNO}_5\text{PdS}$: C 43.87, H 3.68, N 2.33. Found: C 43.69, H 3.73, N 2.31.

[Pd(η^2 -tmetc)(CIN-SMe)]. Yield: 72% (pale yellow microcrystals). IR (KBr pellet): $\nu_{\text{C}=\text{O}}$ 1703.1, $\nu_{\text{C}=\text{N}}$ 1564.9 cm^{-1} . ^1H NMR (CDCl_3 , $T = 298 \text{ K}$, ppm): thiomethyl protons, δ , 2.38 (s, 3H, S- CH_3), methyl ester protons 3.71 (s, 12H, COOCH_3), thiomethyl protons 4.13 (s, 2H, Pyr- CH_2S), pyridine protons 7.40 (d, 1H, H^5_{pyr} , $J = 7.8 \text{ Hz}$), 7.35 (d, 1H, H^3_{pyr} , $J = 7.8 \text{ Hz}$), 7.70 (t, 1H, H^4_{pyr} , $J = 7.7 \text{ Hz}$). ^{13}C NMR (CDCl_3 , $T = 298 \text{ K}$, ppm): pyridine carbons, δ , 159.11 (C^2_{pyr}), 122.32 (C^3_{pyr}), 139.97 (C^4_{pyr}), 124.38 (C^5_{pyr}), thiomethyl carbons 43.35 (Pyr- CH_2S), 19.15 (S- CH_3), methyl carbons 52.64 (COOCH_3), carbonyl carbons 169.97 ($\text{C}=\text{O}$). Anal. Calcd for $\text{C}_{17}\text{H}_{20}\text{ClNO}_5\text{PdS}$: C 37.79, H 3.73, N 2.59. Found: C 37.74, H 3.81, N 2.55.

[Pd(η^2 -tmetc)(CIN-*St*-Bu)]. Yield: 81% (pale yellow microcrystals). IR (KBr pellet): $\nu_{\text{C}=\text{O}}$ 1703.1, $\nu_{\text{C}=\text{N}}$ 1564.9 cm^{-1} . ^1H NMR (CDCl_3 , $T = 298 \text{ K}$, ppm): *tert*-butyl protons, δ , 1.41

(s, 9H, S-C(CH₃)₃), methyl ester protons 3.70 (s, 12H, COOCH₃), thiomethyl protons 4.24 (s, 2H, Pyr-CH₂S), pyridine protons 7.42 (dd, 1H, H⁵_{pyr}, *J* = 7.9; 1.13 Hz), 7.33 (dd, 1H, H³_{pyr}, *J* = 7.6; 0.9 Hz), 7.70 (t, 1H, H⁴_{pyr}, *J* = 7.7 Hz). ¹³C NMR (CDCl₃, *T* = 298 K, ppm): pyridine carbons, δ, 159.98 (C²_{pyr}), 155.10 (C⁶_{pyr}), 121.42 (C³_{pyr}), 140.04 (C⁴_{pyr}), 124.77 (C⁵_{pyr}), thiomethyl carbon 40.10 (Pyr-CH₂S), *tert*-butyl carbons 30.76 (C(CH₃)₃), quaternary *t*-butyl carbon 48.47 (S-C(CH₃)₃), methyl carbons 52.51 (COOCH₃). Anal. Calcd for C₂₀H₂₆ClNO₈PdS: C 41.25, H 4.50, N 2.41. Found: C 41.35, H 4.46, N 2.35.

[Pd(η²-tmetc)(MeN-SMe)]. Yield: 88% (pale yellow microcrystals). IR (KBr pellet): ν_{C=O} 1736.0, 1722.9, ν_{C=N} 1611.0 cm⁻¹. ¹H NMR (CDCl₃, *T* = 298, ppm): thiomethyl protons, δ, 4.17 (s, 2H, CH₂-S), methyl protons, 2.43 (s, 3H, S-CH₃), 2.86 (s, 3H, C-CH₃), methyl ester protons 3.72 (s, 12H, COOCH₃), pyridine protons 7.64 (t, 1H, H⁴_{pyr}, *J* = 7.7 Hz), 7.26 (d, 1H, H³_{pyr}, *J* = 7.7 Hz), 7.21 (d, 1H, H⁵_{pyr}, *J* = 7.7 Hz). Anal. Calcd for C₁₈H₂₃NO₈PdS: C 41.59, H 4.46, N 2.69. Found: C 41.67, H 4.40, N 2.58.

[Pd(η²-tmetc)(MeN-St-Bu)]. Yield: 78% (pale yellow microcrystals). IR (KBr pellet): ν_{C=O}, 1736.0, 1696.5, ν_{C=N}, 1604.4 cm⁻¹. ¹H NMR (CDCl₃, *T* = 298, ppm): thiomethyl protons, δ, 4.21 (s, 2H, CH₂-S), *tert*-butyl protons, 1.37 (s, 9H, S-C(CH₃)₃), methyl protons, 2.84 (s, 3H, C-CH₃); methyl ester protons, 3.71, 3.69 (s, 12H, COOCH₃), pyridine protons, 7.62 (t, 1H, H⁴_{pyr}, *J* = 7.7 Hz), 7.21 (d, 2H H³_{pyr}, H⁵_{pyr}, *J* = 7.7 Hz). Anal. Calcd for C₂₁H₂₉NO₈PdS: C 44.88, H 5.20, N 2.49. Found: C 44.83, H 5.27, N 2.39.

[Pd(η²-tmetc)(DPPQ-Me)]. Yield: 72% (ochre microcrystals). IR (KBr pellet): ν_{C=O}, 1742.6, 1716.3, ν_{C=N}, 1617.6 cm⁻¹. ¹H NMR (CDCl₃, *T* = 298, ppm): methyl protons, δ, 3.22 (s, 3H, C-CH₃); methyl ester protons, 3.71, 3.26 (s, 12H, COOCH₃); phenyl, H⁵_{quin}, H⁷_{quin} protons, 7.54–7.69 (m, 6H); phenyl protons, 7.41 (m, 6H); quinoline protons, 7.87 (t, 1H, H⁶_{quin}, *J* = 7.7 Hz), 7.93 (d, 1H, H³_{quin}, *J* = 9 Hz), 8.22 (d, 1H, H⁴_{quin}, *J* = 9 Hz). ³¹P{¹H} (CDCl₃, *T* = 298, ppm): δ, 25.53. Anal. Calcd for C₃₃H₃₀NO₈PPd: C 55.38, H 4.36, N 2.02. Found: C 55.43, H 4.28, N 2.09.

[Pd(η²-ma)(DPPQ-Me)]. Yield: 86% (pale green microcrystals). IR (KBr pellet): ν_{C=O}, 1772.5.6, 1812.4, ν_{C=N}, 1617.6 cm⁻¹. ¹H NMR (CDCl₃, *T* = 298, ppm): methyl protons, δ, 3.19 (s, 3H, C-CH₃); olefin protons, 4.15 (dd, 1H CH=CH *trans* to P, *J*_{PH} = 10.7, *J*_{HH} = 4.0 Hz), 4.44 (dd, 1H, CH=CH *cis* to P, *J*_{PH} = *J*_{HH} = 4.0 Hz); phenyl protons, 7.44 (m, 10H); quinoline protons, 7.63 (d, 1H, H³_{qui}, *J* = 8.4), 7.65 (d, 1H, H⁷_{qui}, *J* = 7.7 Hz), 7.83 (t, 1H, H⁶_{qui}, *J* = 0.7.7 Hz), 7.99 (d, 1H, H⁵_{qui}, *J* = 7.7 Hz), 8.29 (d, 1H, H⁴_{qui}, *J* = 8.4 Hz). ³¹P{¹H} (CDCl₃, *T* = 298, ppm) δ, 23.01. Anal. Calcd for C₂₆H₂₀NO₃PPd: C 58.72, H 3.79, N 2.63. Found: C 58.81, H 3.70, N 2.59.

Synthesis of the Polymeric Precursors. [PdC₄(COOMe)₄]_n. The complex was prepared according to the published procedure^{4a} by reacting under inert atmosphere (Ar) 0.414 g (0.4 mmol) of Pd₂DBA₃·CHCl₃ suspended in 20 mL of anhydrous acetone with 0.3068 mL (1.25 mmol) of DMA added dropwise. The initially dark suspension was stirred for 1 h at RT, and the resulting yellow solution was treated with activated charcoal. Filtration on a Celite filter, concentration under vacuum, and addition of diethyl ether yields 0.282 g (0.72 mmol) of the title complex as yellow microcrystals. Yield: 90%. IR (KBr pellet): ν_{C=O} 1730.0, 1700.0, ν_{C-H}, 2960.0 cm⁻¹.

The following complexes were prepared in an analogous way using the appropriate alkynes.

[PdC₄(COOEt)₄]_n. Yield: 96% (yellow microcrystals). IR (KBr pellet): ν_{C=O} 1716.0, 1690.0, ν_{C-H} 2986.0 cm⁻¹.

[PdC₄(COOt-Bu)₄]_n. Yield: 91% (yellow microcrystals). IR (KBr pellet): ν_{C=O} 1709.0, 1678.0, ν_{C-H} 2986.5 cm⁻¹.

Synthesis of the Palladacyclopentadienyl Derivatives. [PdC₄(COOMe)₄(HN-SMe)]. To 0.0685 g (0.46 mmol) of the ligand HN-SMe dissolved in 15 mL of anhydrous acetone was added 0.164 g (0.41 mmol) of [PdC₄(COOMe)₄]_n under inert

atmosphere. The resulting solution was stirred for 2 h at RT and concentrated under vacuum. Addition of diethyl ether (20 mL) yields 0.2101 g (0.38 mmol) of the title substrate as pale yellow microcrystals. The complex was filtered, washed with diethyl ether, and dried in a desiccator. Yield: 94%. IR (KBr pellet): ν_{C=O} 1722.9, 1689.9, ν_{C=N} 1611.0, ν_{C-H} 2953.6 cm⁻¹. ¹H NMR (CDCl₃, *T* = 298 K, ppm): methyl protons, δ, 2.24 (s, 3H, S-CH₃), methyl ester protons, 3.65 (s, 3H, COOCH₃), 3.70 (s, 3H, COOCH₃), thiomethyl protons 4.11 (s, 2H, pyr-CH₂S), pyridine protons 7.41 (td, 1H, H⁵_{pyr}, *J*_{ortho5-4} = 7.5 Hz, *J*_{meta5-3} = 1.4 Hz), 7.5 (d, 1H, H³_{pyr}, *J*_{ortho3-4} = 7.7 Hz), 7.88 (td, 1H, H⁴_{pyr}, *J*_{meta4-6} = 1.7 Hz), 8.65 (dd, 1H, H⁶_{pyr}, *J*_{ortho6-5} = 5.6 Hz). ¹³C NMR (CDCl₃, *T* = 298 K, ppm): methyl carbon, δ, 18.59 (S-CH₃), thiomethyl carbons 43.42 (pyr-CH₂-S), methyl carbons 51.51, 51.76 (COOC^αH₃), 51.91 (COOC^βH₃), pyridine carbons 124.67 (C⁵_{pyr}), 124.97 (C³_{pyr}), 139.67 (C⁴_{pyr}), 152.46 (C⁶_{pyr}), 159.95 (C²_{pyr}), cyclo-butadienyl carbons 144.36, 149.02 (C^β=C), 158.14, 169.23 (C^α=C), carbonyl carbons 164.14, 165.30 (C^βOOCH₃), 173.66, 173.94 (C^αOOCH₃). Anal. Calcd for C₁₉H₂₁NO₈PdS: C 43.07, H 3.99, N 2.64. Found: C 42.98, H 3.96, N 2.59.

The following complexes were prepared in an analogous way using the appropriate ligands.

[PdC₄(COOMe)₄(HN-SPh)]. Yield: 93% (pale yellow microcrystals). IR (KBr pellet): ν_{C=O} 1722.9, 1689.9, ν_{C=N} 1611.0, ν_{C-H} 2953.6 cm⁻¹. ¹H NMR (CDCl₃, *T* = 298 K, ppm): methyl ester protons, δ, 3.38 (s, 3H, COOCH₃), 3.65 (s, 3H, COOCH₃), 3.71 (s, 6H, COOCH₃); thiomethyl protons, 4.42 (s, 2H, pyr-CH₂S), phenyl protons, 7.3 (m, 5H, S-Ph), pyridine protons 7.64 (m, 1H, H⁵_{pyr}, *J*_{ortho5-4} = 7.5 Hz, *J*_{meta5-3} = 1.4 Hz), 7.67 (m, 1H, H³_{pyr}, *J*_{ortho3-4} = 7.7 Hz), 7.75 (td, 1H, H⁴_{pyr}, *J*_{meta4-6} = 1.7 Hz), 8.63 (dd, 1H, H⁶_{pyr}, *J*_{ortho6-5} = 5.5 Hz). ¹³C NMR (CDCl₃, *T* = 298 K, ppm): thiomethyl carbons, δ, 47.53 (pyr-CH₂-S), methyl carbons 51.49 (COOC^αH₃), 51.94 (COOC^βH₃), pyridine carbons 124.32 (C⁵_{pyr}), 124.54 (C³_{pyr}), 139.49 (C⁴_{pyr}), 152.15 (C⁶_{pyr}), 159.36 (C²_{pyr}), phenyl carbons 129.83, 130.02, 130.54, 133.58 (S-C₆H₅) cyclobutadienyl carbons 144.69, 149.02 (C^β=C), 164.17, 165.35 (C^α=C), carbonyl carbons 159.42, 168.70 (C^βOOCH₃), 173.02, 173.72 (C^αOOCH₃). Anal. Calcd for C₂₄H₂₃NO₈PdS: C 48.70, H 3.92, N 2.37. Found: C 48.76, H 3.89, N 2.40.

[PdC₄(COOMe)₄(HN-St-Bu)]. Yield: 91% (pale yellow microcrystals). IR (KBr pellet): ν_{C=O} 1722.9, 1689.9, ν_{C=N} 1611.0, ν_{C-H} 2953.6 cm⁻¹. ¹H NMR (CDCl₃, *T* = 298 K, ppm): methyl protons, δ, 1.18 (s, 9H, S-(CH₃)₃), methyl ester protons, 3.60 (s, 3H, COOCH₃), 3.68 (s, 3H, COOCH₃), 3.69 (s, 3H, COOCH₃), 3.72 (s, 3H, COOCH₃), thiomethyl protons 4.27 (s, 2H, pyr-CH₂S), pyridine protons 7.38 (t, 1H, H⁵_{pyr}, *J*_{ortho5-4} = 7.7 Hz), 7.5 (d, 1H, H³_{pyr}, *J*_{ortho3-4} = 7.7 Hz), 7.87 (td, 1H, H⁴_{pyr}, *J*_{ortho4-3} = 7.7 Hz, *J*_{meta4-6} = 1.7 Hz), 8.60 (d, 1H, H⁶_{pyr}, *J*_{ortho6-5} = 5.5 Hz). ¹³C NMR (CDCl₃, *T* = 298 K, ppm): methyl carbons, δ, 31.19 (S-C(CH₃)₃), thiomethyl carbons 40.49 (pyr-CH₂-S), *tert*-butyl carbon 40.49 (S-C(CH₃)₃), methyl carbons 51.44 (COOC^αH₃), 51.78 (COOC^βH₃), pyridine carbons 123.66 (C³_{pyr}), 124.37 (C⁵_{pyr}), 139.83 (C⁴_{pyr}), 151.88 (C⁶_{pyr}), 161.34 (C²_{pyr}), cyclobutadienyl carbons 144.96, 145.73 (C^β=C), 160.02, 165.26 (C^α=C), carbonyl carbons 164.36, 164.69 (C^βOOCH₃), 173.75, 173.27 (C^αOOCH₃). Anal. Calcd for C₂₂H₂₇NO₈PdS: C 46.20, H 4.76, N 2.45. Found: C 46.19, H 4.66, N 2.51.

[PdC₄(COOMe)₄(MeN-SMe)]. Yield: 91% (pale yellow microcrystals). IR (KBr pellet): ν_{C=O} 1703.1, ν_{C=N} 1611.0, ν_{C-H} 2953.6 cm⁻¹. ¹H NMR (CDCl₃, *T* = 298 K, ppm): methyl protons, δ, 2.15 (s, 3H, S-CH₃), methyl protons, 2.80 (s, 3H, pyr-CH₃), methyl ester protons, 3.55 (s, 6H, COOCH₃), 3.71 (s, 6H, COOCH₃), thiomethyl protons 4.28 (s, 2H, pyr-CH₂S), pyridine protons 7.26 (s, 2H, H⁵_{pyr}), 7.5 (d, 1H, H³_{pyr}, H⁴_{pyr}), 7.72 (t, 1H, *J*_{ortho} = 9 Hz). ¹³C NMR (CDCl₃, *T* = 298 K, ppm): methyl carbon, δ, 17.59 (S-CH₃), methyl carbon 27.88 (pyr-CH₃), thiomethyl carbons 43.42 (pyr-CH₂-S), methyl carbons 51.50 (COOC^αH₃), 51.98 (COOC^βH₃), pyridine carbons 121.60 (C⁵_{pyr}), 124.57 (C³_{pyr}), 139.10 (C⁴_{pyr}), 157.12 (C⁶_{pyr}), 162.58

(C²_{pyr}), cyclobutadienyl carbons 148 (C^β=C), 165 (C=C), carbonyl carbons 165.10 (C^βOOCH₃), 173.39 (C^αOOCH₃). Anal. Calcd for C₂₀H₂₃NO₈PdS: C 44.17, H 4.26, N 2.58. Found: C 44.24, H 4.22, N 2.63.

[PdC₄(COOMe)₄(MeN-SPh)]. Yield: 66% (pale yellow microcrystals). IR (KBr pellet): ν_{C=O} 1703.1, ν_{C=N} 1611.0, ν_{C-H} 2953.6 cm⁻¹. ¹H NMR (CDCl₃, T = 298 K, ppm): methyl protons, δ, 2.81 (s, 3H, pyr-CH₃), methyl ester protons 3.43 (s, 6H, COOCH₃), 3.72 (s, 6H, COOCH₃); thiomethyl protons, 4.61 (s, 2H, pyr-CH₂S), phenyl protons, 7.26 (m, 3H, S-Ph), 7.57 (m, 2H, S-Ph), pyridine protons 7.64 (d, 1H, H⁵_{pyr}, J_{ortho5-4} = 7.6 Hz), 7.08 (d, 1H, H³_{pyr}, J_{ortho3-4} = 7.6 Hz), 7.60 (m, 1H, H⁴_{pyr}). ¹³C NMR (CDCl₃, T = 298 K, ppm): methyl carbons, δ, 27.42 (pyr-CH₃), thiomethyl carbons, 46.89 (pyr-CH₂-S), methyl carbons 51.47 (COOCH₃), 51.98 (COOCH₃), pyridine carbons 121.19 (C³_{pyr}), 124.26 (C⁵_{pyr}), 138.89 (C⁴_{pyr}), 156.92 (C²_{pyr}), 161.93 (C²_{pyr}), phenyl carbons 129.84, 132.62, (S-C₆H₅), cyclobutadienyl carbons 147.31 (C^β=C), 167.06 (C^α=C), carbonyl carbons 164.91 (C^βOOCH₃), 173.44 (C^αOOCH₃). Anal. Calcd for C₂₅H₂₅NO₈PdS: C 49.55, H 4.16, N 2.31. Found: C 49.61, H 4.17, N 2.35.

[PdC₄(COOMe)₄(MeN-St-Bu)]. Yield: 91% (pale yellow microcrystals). IR (in KBr) (cm⁻¹): ν_{C=O} 1703.1, ν_{C=N} 1611.0, ν_{C-H} 2947.0 cm⁻¹. ¹H NMR (CDCl₃, T = 298 K, ppm): methyl protons, δ, 1.13 (s, 9H, S-(CH₃)₃), methyl protons 2.79 (s, 3H, pyr-CH₃), methyl ester protons, 3.31 (s, 3H, COOCH₃), 3.74 (s, 3H, COOCH₃), 3.70 (s, 6H, COOCH₃), thiomethyl protons 4.41 (s, 2H, pyr-CH₂S), pyridine protons 7.24, 7.26 (2d, 2H, H⁵_{pyr}, H³_{pyr}, J_{meta} = 4.15 Hz), 7.71 (t, 1H, H⁴_{pyr}, J_{ortho} = 7.7 Hz). ¹³C NMR (CDCl₃, T = 298 K, ppm): methyl carbon, δ, 27.47 (pyr-CH₃), 31.27 (S-C(CH₃)₃), thiomethyl carbons 41.36 (pyr-CH₂-S), *tert*-butyl carbon 49.71 (S-C(CH₃)₃), methyl carbons 51.17, 51.52 (COOCH₃), 51.90 (COOCH₃), pyridine carbons 120.24 (C⁵_{pyr}), 124.29 (C³_{pyr}), 139.30 (C⁴_{pyr}), 158.62 (C⁶_{pyr}), 161.94 (C²_{pyr}), cyclobutadienyl carbons 155.13 (C^β=C), 163.20, 171.07 (C^α=C), carbonyl carbons 166.62 (C^βOOCH₃), 172.13, 174.96 (C^αOOCH₃). Anal. Calcd for C₂₃H₂₉NO₈PdS: C 47.17, H 4.99, N 2.39. Found: C 47.12, H 4.90, N 2.33.

[PdC₄(COOMe)₄(CIN-SMe)]. Yield: 91% (pale yellow microcrystals). IR (KBr pellet): ν_{C=O} 1703.1, ν_{C=N} 1584.6 cm⁻¹. ¹H NMR (CDCl₃, T = 298 K, ppm): methyl protons, δ, 2.17 (s, 3H, CH₃-S), methyl ester protons 3.60 (bs, 6H, Pd-C=C-COOCH₃), 3.72 (s, 6H, Pd-C-COOCH₃), thiomethyl protons 4.32 (s, 2H, pyr-CH₂S), pyridine protons 7.43 (d, 1H, H³_{pyr}, J = 7.7 Hz), 7.43 (d, 1H, H⁵_{pyr}, J = 7.7 Hz), 7.80 (t, 1H, H⁴_{pyr}, J = 7.7 Hz). Anal. Calcd for C₁₅H₂₀ClNO₈PdS: C 40.44, H 3.57, N 2.48. Found: C 40.39, H 3.62, N 2.43.

[PdC₄(COOMe)₄(CIN-SPh)]. Yield: 80% (pale yellow microcrystals). IR (KBr pellet): ν_{C=O}, 1703.1; ν_{C=N}, 1584.6 cm⁻¹. ¹H NMR (CDCl₃, T = 298 K, ppm): methyl ester protons, δ, 3.49 (s, 6H, Pd-C=C-COOCH₃), 3.72 (s, 6H, Pd-C-COOCH₃), thiomethylene protons 4.63 (bs, 2H, pyr-CH₂S), aromatic protons 7.25–7.35 (m, 4H, 2H_{ortho}, 1H_{para}, H⁵_{pyr}), 7.21 (d, 1H, H³_{pyr}, J = 7.7 Hz), 7.63 (t, 1H, H⁴_{pyr}, J = 7.7 Hz), 7.55–7.65 (m, 2H, 2H_{meta}). Anal. Calcd for C₂₄H₂₂ClNO₈PdS: C 46.02, H 3.54, N 2.24. Found: C 46.09, H 3.58, N 2.19.

[PdC₄(COOMe)₄(CIN-St-Bu)]. Yield: 90% (pale yellow microcrystals). IR (KBr pellet): ν_{C=O} 1703.1, ν_{C=N}, 1564.9 cm⁻¹. ¹H NMR (CDCl₃, T = 298 K, ppm): *tert*-butyl protons, δ, 1.17 (s, 9H, S-C(CH₃)₃), methyl ester protons 3.59 (bs, 6H, Pd-C=C-COOCH₃), 3.71 (s, 6H, Pd-C-COOCH₃), thiomethylene protons 4.46 (s, 2H, pyr-CH₂S), pyridine protons 7.41 (d, 1H, H⁵_{pyr}, J = 7.7 Hz), 7.42 (d, 1H, H³_{pyr}, J = 7.7 Hz), 7.80 (t, 1H, H⁴_{pyr}, J = 7.8 Hz). Anal. Calcd for C₂₂H₂₆ClNO₈PdS: C 43.58, H 4.32, N 2.31. Found: C 43.62, H 4.35, N 2.28.

[PdC₄(COOMe)₄(TMQ-Me)]. Yield: 86% (pale yellow microcrystals). IR (KBr pellet): ν_{C=O} 1703.1, ν_{C=N} 1564.9 cm⁻¹. ¹H NMR (CDCl₃, T = 298 K, ppm): thiomethyl protons, δ, 2.73 (s, 3H, S-CH₃), methyl protons, 2.97 (s, 3H, qui-CH₃), methyl ester protons, 3.60 (bs, 6H, Pd-C=C-COOCH₃), 3.72 (s, 6H, Pd-C-COOCH₃), quinoline protons 7.49 (d, 1H, H⁶_{qui}, d, J =

8.5 Hz), 7.58 (t, 1H, H⁶_{qui}, J = 7.6 Hz), 7.80–8.00 (bm, 2H, H⁵_{qui}, H⁷_{qui}), 8.25 (d, 1H, H⁴_{qui}, J = 7.7). Anal. Calcd for C₂₃H₂₃NO₈PdS: C 47.64, H 4.00, N 2.42. Found: C 47.66, H 4.05, N 2.38.

[PdC₄(COOMe)₄(DPPQ-Me)]. Yield: 87% (orange microcrystals). IR (KBr pellet): ν_{C=O} 1729.4, 1696.5, ν_{C=N} 1611.0 cm⁻¹. ¹H NMR (CDCl₃, T = 298 K, ppm): methyl protons, δ, 3.39 (s, 3H, C-CH₃), methyl ester protons 3.68 (s, 3H, Pd-C=C-COOCH₃), 3.64 (s, 3H, Pd-C-COOCH₃), 2.89 (s, 3H, Pd-C-COOCH₃), 2.86 (s, 3H, Pd-C-COOCH₃); quinoline protons 7.89 (d, 1H, H³_{qui}, d, J = 9 Hz), 8.18 (d, 1H, H⁴_{qui}, J = 9 Hz); phenyl protons 7.42 (m, 10H). ³¹P{¹H} (CDCl₃, T = 298, ppm) δ, 30.16. Anal. Calcd for C₃₄H₃₀NO₈PPd: C 56.88, H 4.21, N 1.95. Found: C 56.94, H 4.15, N 2.01.

[PdC₄(COOEt)₄(DPPQ-Me)]. Yield: 47% (red-orange microcrystals). IR (KBr pellet): ν_{C=O} 1722.9, 1696.5, ν_{C=N} 1611.0 cm⁻¹. ¹H NMR (CDCl₃, T = 298 K, ppm): methyl protons, δ, 2.91 (s, 3H, C-CH₃); ethyl ester protons 1.23 (t, 3H, Pd-C=C-COOCH₂CH₃), 1.22 (t, 3H, Pd-C-COOCH₂CH₃), 1.00 (t, 3H, Pd-C-COOCH₂CH₃), 0.85 (t, 3H, Pd-C-COOCH₂CH₃), 4.11 (bm, 4H, Pd-C-COOCH₂CH₃), 3.77 (bm, 3H, Pd-C-COOCH₂CH₃); quinoline protons, 7.87 (d, 1H, H³_{qui}, d, J = 9 Hz), 8.17 (d, 1H, H⁴_{qui}, J = 9 Hz); phenyl protons 7.42 (m, 10H). ³¹P{¹H} (CDCl₃, T = 298, ppm) δ, 30.31. Anal. Calcd for C₃₈H₂₈NO₈PPd: C 59.74, H 3.69, N 1.83. Found: C 59.83, H 3.59, N 1.78.

[PdC₄(COO*t*-Bu)₄(DPPQ-Me)]. Yield: 86% (yellow microcrystals). IR (KBr pellet): ν_{C=O} 1702.9, 1683.7, ν_{C=N} 1611.0 cm⁻¹. ¹H NMR (CDCl₃, T = 298 K, ppm): methyl protons, δ, 3.11 (s, 3H, C-CH₃), *tert*-butyl protons, 1.51 (s, 9H, C(CH₃)₃), 1.50 (s, 9H, C(CH₃)₃), 1.04 (s, 9H, C(CH₃)₃), 0.97 (s, 9H, C(CH₃)₃); quinoline protons 7.83 (d, 1H, H³_{qui}, d, J = 9 Hz), 8.11 (d, 1H, H⁴_{qui}, J = 9 Hz); phenyl protons 7.53–7.33 (m, 10H). ³¹P{¹H} (CDCl₃, T = 298, ppm) δ, 25.79. Anal. Calcd for C₄₆H₅₄NO₈PPd: C 62.34, H 6.14, N 1.58. Found: C 62.41, H 6.15, N 1.64.

[PdC₄(COOMe)₄(SNS(Me))]. Yield: 58% (yellow microcrystals). IR (KBr pellet): ν_{C=O} 1703.1, 1676.8, ν_{C=N} 1611.0, ν_{C-H} 2953.6 cm⁻¹. ¹H NMR (CDCl₃, T = 298 K, ppm): methyl protons, δ, 2.17 (s, 6H, S-CH₃), methyl ester protons, 3.54 (s, 6H, COOCH₃), 3.72 (s, 6H, COOCH₃); thiomethyl protons 4.21 (s, 4H, pyr-CH₂S), pyridine protons 7.39 (d, 2H, H⁵_{pyr}, H³_{pyr}), 7.82 (t, 1H, H⁴_{pyr}, J_{ortho} = 7.7 Hz). ¹³C NMR (CDCl₃, T = 298 K, ppm): methyl carbon, δ, 16.98 (S-CH₃), thiomethyl carbons 43.50 (pyr-CH₂-S), methyl carbons 51.56 (COOCH₃), 51.98 (COOCH₃), pyridine carbons 123.26 (C⁵_{pyr}, C³_{pyr}), 160.12 (C²_{pyr}, C⁶_{pyr}), cyclobutadienyl carbons 148.00 (C^β=C), 163.20 (C^α=C), carbonyl carbons 165.04 (C^βOOCH₃), 173.08 (C^αOOCH₃). Anal. Calcd for C₂₁H₂₅NO₈PdS₂: C 42.75, H 4.27, N 2.37. Found: C 42.79, H 4.23, N 2.31.

[PdC₄(COOMe)₄(SNS(Ph))]. Yield: 79% (pale yellow microcrystals). IR (KBr pellet): ν_{C=O} 1716.3, 1736, 1676.8, ν_{C=N} 1611.0, ν_{C-H}, 2960.1 cm⁻¹. ¹H NMR (CDCl₃, T = 298 K, ppm): methyl ester protons, δ, 3.39 (s, 6H, COOCH₃), 3.74 (s, 6H, COOCH₃); thiomethyl protons 4.55 (s, 4H, pyr-CH₂S), phenyl protons 7.35 (m, 10H, S-Ph), pyridine protons 7.10 (d, 2H, H⁵_{pyr}, H³_{pyr}), 7.56 (t, 1H, H⁴_{pyr}, J_{ortho} = 7.7 Hz). Anal. Calcd for C₃₁H₂₉NO₈PdS₂: C 52.14, H 4.09, N 1.96. Found: C 52.23, H 4.12, N 2.02.

[PdC₄(COOMe)₄(SNS(*t*-Bu))]. Yield: 75% (pale yellow microcrystals). IR (KBr pellet): ν_{C=O} 1722.1, 1607, ν_{C=N} 1611.0, ν_{C-H}, 2976.2 cm⁻¹. ¹H NMR (CDCl₃, T = 298 K, ppm): methyl protons, δ, 1.33 (s, 12H, S-C(CH₃)₃), methyl ester protons 3.30 (s, 6H, COOCH₃), 3.73 (s, 6H, COOCH₃); thiomethyl protons 4.34 (s, 4H, pyr-CH₂S), pyridine protons 7.36 (d, 2H, H⁵_{pyr}, H³_{pyr}), 7.75 (t, 1H, H⁴_{pyr}, J_{ortho} = 7.7 Hz). Anal. Calcd for C₂₆H₃₃NO₈PdS₂: C 47.45, H 5.05, N 2.13. Found: C 47.50, H 5.00, N 2.15.

[PdC₄(COOEt)₄(HN-SMe)]. In the synthesis of the title complex *n*-hexane instead of diethyl ether is used as precipitant. Yield: 77% (yellow microcrystals). IR (KBr pellet): ν_{C=O} 1709.7, ν_{C=N} 1611.0, ν_{C-H} 2953.6 cm⁻¹. ¹H NMR (CDCl₃, T = 298 K, ppm): methyl protons, δ, 1.25 (m, 12 H, COO-CH₂-

CH_3), methyl protons 2.23 (s, 3H, S- CH_3), methylene protons 4.15 (m, 10H, pyr- CH_2S , COO- $\text{CH}_2\text{-CH}_3$), pyridine protons 7.39 (t, 1H, H^5_{pyr} , $J_{\text{ortho4-5}} = 7.7$ Hz), 7.49 (d, 1H, H^3_{pyr} , $J_{\text{ortho3-4}} = 7.7$ Hz), 7.87 (td, 1H, H^4_{pyr} , $J_{\text{meta4-6}} = 1.5$ Hz), 8.62 (d, 1H, H^6_{pyr} , $J_{\text{ortho6-5}} = 4.9$ Hz). Anal. Calcd for $\text{C}_{23}\text{H}_{29}\text{NO}_8\text{PdS}$: C 47.17, H 4.99, N 2.39. Found: 47.20, H 5.03, N 2.34.

[PdC₄(COO*t*-Bu)₄(HN-SMe)]. In the synthesis of the title complex *n*-hexane instead of diethyl ether is used as precipitant. Yield: 49% (dark yellow oily product). IR (KBr pellet): $\nu_{\text{C=O}}$ 1709.7, $\nu_{\text{C=N}}$ 1611.0, $\nu_{\text{C-H}}$ 2953.6 cm^{-1} . ^1H NMR (CDCl_3 , $T = 298$ K, ppm): methyl protons, δ , 1.38, 1.50, 1.51, 1.52 (4s, 36 H, COO-C(CH_3)₃), methyl protons 2.16 (s, 3H, S- CH_3), thiomethyl protons 4.24 (s, 2H, pyr- CH_2S), pyridine protons

7.35 (t, 1H, H^5_{pyr} , $J_{\text{ortho4-5}} = 7.7$ Hz), 7.47 (d, 1H, H^3_{pyr} , $J_{\text{ortho3-4}} = 7.7$ Hz), 7.84 (td, 1H, H^4_{pyr} , $J_{\text{meta4-6}} = 1.6$ Hz), 8.95 (d, 1H, H^6_{pyr} , $J_{\text{ortho6-5}} = 5.3$ Hz). Anal. Calcd for $\text{C}_{31}\text{H}_{45}\text{NO}_8\text{PdS}$: C 53.33, H 6.50, N 2.01. Found: C 53.27, H 6.45, N 2.12.

Supporting Information Available: Table 1 Si (summary of crystal and refinement data) and Table 2 Si (selected bond distances and angles of the two complexes). Equilibrium constant determination, nonlinear regression analysis, and simulation details. This material is available free of charge via the Internet at <http://pubs.acs.org>.

OM058036T